Synthetic Extracellular Matrices for In Situ Tissue Engineering

Alison B. Pratt,[1,2,3] Franz E. Weber,[4] Hugo G. Schmoekel,[1]* Ralph Müller,[1] Jeffrey A. Hubbell[1,2]

[1]Institute for Biomedical Engineering, Swiss Federal Institute of Technology (ETH) and University of Zurich, Moussonstrasse 18, CH-8044 Zurich, Switzerland; telephone: + 41 1 632 45 85; fax: + 41 1 632 12 14; e-mail: hubbell@biomed.mat.ethz.ch
[2]Department of Materials, Swiss Federal Institute of Technology (ETH), CH-8044 Zurich, Switzerland
[3]Division of Chemistry and Chemical Engineering, California Institute of Technology, Pasadena, California
[4]Department of Cranio-maxillofacial Surgery, University Hospital Zurich, CH-8091 Zurich, Switzerland

Received 8 July 2003; accepted 8 October 2003

Published online 12 February 2004 in Wiley InterScience (www.interscience.wiley.com). DOI: 10.1002/bit.10897

Abstract: Cell interactions with the extracellular matrix play important roles in guiding tissue morphogenesis. The matrix stimulates cells to influence such things as differentiation and the cells actively remodel the matrix via local proteolytic activity. We have designed synthetic hydrogel networks that participate in this interplay: They signal cells via bound adhesion and growth factors, and they also respond to the remodeling influence of cell-associated proteases. Poly(ethylene glycol)-bis-vinylsulfone was crosslinked by a Michael-type addition reaction with a peptide containing three cysteine residues, the peptide sequence being cleavable between each cysteine residue by the cell-associated protease plasmin. Cells were able to invade gel networks that contained adhesion peptides and were crosslinked by plasmin-sensitive peptides, while materials lacking either of these two characteristics resisted cell infiltration. Incorporated bone morphogenetic protein-2 (BMP-2) induced bone healing in a rat model in materials that were both adhesive and plasmin-sensitive, while materials lacking plasmin sensitivity resisted formation of bone within the material. Furthermore, when a heparin bridge was incorporated as a BMP-2 affinity site, mimicking yet another characteristic of the extracellular matrix, statistically improved bone regeneration was observed.

Keywords: matrix; proteolysis; peptide; growth factor; bone

In vivo, cells interact in a bidirectional and dynamic manner with their extracellular matrices. The matrix stimulates cells via adhesion factors (Howe et al., 1998; Huttenlocher et al., 1995; Maheshwari et al., 2000; Palecek et al., 1997; Yamada and Kleinman, 1992) and bound growth factors (Reddi, 2000; Ruppert et al., 1996; Sieron et al., 2002), and cells enzymatically remodel the matrix to release the bound growth factors (Chang and Werb, 2001; Sternlicht and Werb, 2001) and clear a path to enable cell migration (Chen, 1992; Murphy and Gavrilovic, 1999; Sternlicht and Werb, 2001; Streuli, 1999; Vu and Werb, 2000; Werb, 1997). Despite the importance of such interactions in tissue morphogenesis, this concept of two-way communication between cells and their matrix has just begun to be explored in synthetic materials for tissue engineering. While some biological materials possess these characteristics naturally, such as bovine-derived collagen (Howell et al., 1997) and human-derived fibrin(ogen) (Horch et al. 2001; Hunziker et al. 2002), their clinical use carries potential risks of disease transmission and immunogenicity. A specific case in point is the use of collagen from bovine bone to deliver recombinant human bone morphogenetic factor-7 in human patients; in this study, 5% of patients were observed to develop anti-bovine collagen antibodies and 10% anti-rhBMP-7 antibodies (European Agency for the Evaluation of Medicinal Products, 2001; Friedlaender et al., 2001). Thus, there exists a strong motivation to develop synthetic analogs to such natural materials.

Our group has designed synthetic materials as biomimetic matrices with four key characteristics in mind: (1) in situ transformation from liquids to solids, (2) susceptibility to the enzymatic matrix remodeling capacity of migrating cells, (3) presentation of adhesion ligands to cells, and (4) incorporation of affinity sites for growth factor binding. The first characteristic permits administration using a minimally invasive surgical technique; the second and third together allow cell invasion and remodeling of the material, using the same mechanisms as for biologically derived materials; and the fourth allows cellular remodeling processes to mobilize

Correspondence to: Jeffrey A. Hubbell
*Present address: Clinic for Small Animals, Department of Veterinary Medicine, University of Bern, CH-3001 Bern, Switzerland
Contract grant sponsor: Swiss National Science Foundation

growth factor morphogens, also using the same mechanisms as occur in the natural extracellular matrix.

We obtained the characteristic of in situ transformation from liquids to elastic hydrogel networks by mixing a mutually reactive pair of macromolecular precursors immediately prior to administration. We selected a Michael-type conjugate addition reaction of a thiol on a peptide macromer with a vinylsulfone on a polymeric macromer (Elbert et al., 2001; Lutolf and Hubbell, 2003; Lutolf et al., 2003). This reaction is relatively selective in the extracellular biological environment (Elbert and Hubbell, 2001; Lutolf et al., 2001), due to the scarcity of sterically accessible, unpaired cysteine residues in the oxidizing environment of extracellular fluids, and the rare occurrence of conjugated unsaturations in biological molecules. While amines are also capable of conjugate addition to the vinylsulfone, the pK_a of most amines is far from physiological pH, thus strongly favoring reaction with the thiol macromer (Morpurgo et al., 1996). Although low-molecular-weight vinylsulfones are known to demonstrate toxicity (Dearfield et al., 1991), coupling to a water-soluble polymer prevents their entry into the cytoplasm and toxic reactions with glutathione and DNA.

We obtained cell invasion into the hydrogel networks by incorporating two biological recognition characteristics: sensitivity to cell-associated proteases and binding to cell-surface adhesion receptors. While cells invade and remodel the natural extracellular matrix by creating their own pores via cell–surface proteases, most designs for biomaterials do not accommodate this. Common polymers used as tissue engineering scaffolds, such as poly(lactic acid) and related polyesters, must include preformed pores to permit cell migration (Lu et al., 2000; Shastri et al., 2000; Wake et al., 1994). Our group (West and Hubbell, 1999) as well as Gobin and West (Gobin and West, 2002) have recently described photopolymerizable macromers with protease substrates in the main chain, to allow degradation by cellular proteases. Our group has described an operationally simpler design, in which a vinylsulfone-terminated polymer is crosslinked with a cysteine-containing protease substrate peptide; proteolytic cleavage of the crosslinking peptide induces degradation of the network (Lutolf and Hubbell, 2003; Lutolf et al., 2003). As the polymer, we selected poly(ethylene glycol) (PEG) because of its biocompatibility and low toxicity (Abuchowski et al., 1977; Harris, 1992). As a crosslinking peptide, in this work we utilized a sequence that can be cleaved by plasmin that is activated at the surfaces of most migrating cells (Anand et al., 1995; Chen, 1992; Fibbi et al., 1999). To achieve the second characteristic of binding of cell-surface adhesion receptors, we incorporated a GRGDSP peptide sequence capable of binding to the integrin family of receptors, which transmits stress from the cytoskeleton through the membrane to adhesion proteins in the extracellular matrix (Hern and Hubbell, 1998; Howe et al., 1998; Huttenlocher et al., 1995; Lutolf and Hubbell, 2003; Lutolf et al., 2003; Massia and Hubbell, 1991). The adhesion peptide was incorporated dangling upon the terminus of a soluble polymer (Elbert and Hubbell, 2001)—this has been shown to be beneficial (Hern and Hubbell, 1998).

As a final characteristic of our design, one of the key features of this study, we provided affinity sites within the hydrogel network for binding of growth factor morphogens. Most growth factors bind to heparan sulfate proteoglycans in the natural extracellular matrix (Ruppert et al., 1996; Sakiyama-Elbert and Hubbell, 2000a, 2000b), and we mimicked this by attaching a heparin-binding peptide to the network, providing binding sites for heparin-binding growth factors via a heparin bridge (Sakiyama-Elbert and Hubbell 2000a; 2000b). Our group has previously demonstrated, both on theoretical grounds and experimentally, that heparin bound in such a manner can substantially delay the release of even very weakly binding growth factors (Sakiyama-Elbert and Hubbell 2000a; 2000b).

METHODS

Hydrogel Design

Hydrogels were formed from liquid precursors by reaction of a difunctional PEG-bis-vinylsulfone with a tricysteine-containing peptide, the peptide possessing a plasmin-substrate site between each cysteine. Thus, reaction of the two precursors yielded a network of PEG crosslinked with the plasmin-sensitive peptide, and exposure to plasmin should yield soluble PEG terminally functionalized with a peptide fragment. As the crosslinking peptide, we selected GCYKNRCGYKNRCG-NH_2 (plasmin substrate site underlined, vinylsulfone-reactive site shown in bold). Plasmin

Table I. Plasmin-substrate specificity.[a]

P2	P1	P1′	P2′	Effect
Try, Phe, Trp				Enhance hydrolysis
Lys, Arg, His				Slow hydrolysis
	Lys, Arg			Required for hydrolysis
		Ser, Thr		Enhance hydrolysis
		Pro		Prevents hydrolysis
			Gly, Ala, Val	Enhance hydrolysis
			Ser, Thr, Glu, Asp	Slow hydrolysis

[a]Kiel (1992).

is an endopeptidase that cleaves carboxy-terminal to Lys- or Arg- residues. Plasmin's substrate specificity depends on the amino acid residues surrounding the Lys- or Arg-peptide bond (Table I) (Kiel, 1992). The rate of proteolysis is significantly affected by the P4, P2, P1, P1′, and P2′ residues (Schechter and Berger, 1967), while it is relatively insensitive in the P3 substrate position (Backes et al., 2000). Plasmin substrate sites reported in fibrinogen were evaluated as potential substrate sites in the crosslinker peptide (Table II). In our selection of a substrate, Lys was favored over Arg in the P1 position, since Lys is kinetically favored by plasmin and also confers substrate specificity to plasmin over other serine proteases, such as thrombin. Solubility was also considered, using the grand average of the hydropathicity (GRAVY) index as a predictive tool (Expert Protein Analysis System ExPASy SWISS-PROT database,www.expasy.ch/tools/protparam.html; (Kyte and Doolittle, 1982) (Table III). Relatively hydrophobic sequences (GRAVY > 0) were eliminated, and some amino acids were disfavored. Met was considered undesirable for synthetic reasons, Gln was disfavored for solubility reasons (Kyte and Doolittle, 1982), and Lys outside of P1 was avoided to favor only one plasmin(ogen) binding and cleavage site per peptide. Tyr was chosen for the P2 site since it is known to have a favorable effect on plasmin-substrate kinetics in that position (Table I). GRAVY values calculated for the remaining possible combinations of P1′–P3′ amino acids indicated that Asn would be less favorable than Arg and that Ser would be less favorable for solubility than Asn and Asp. Among the remaining residues, no preference was given, and the substrate was selected as CYKNRDC. Because of a negative influence of the D residue on the reactivity of the C thiol toward vinylsulfone (Lutolf et al., 2001), this residue was eliminated from the final crosslinking peptide design. To impart cell adhesion character, the monocysteine adhesion peptide *N*-acetyl-GCYGRGDSPG-NH_2 was utilized (adhesion domain underlined) (Hern and Hubbell, 1998; Pierschbacher and Ruoslahti, 1984). To impart heparin-binding character, the monocysteine heparin-binding peptide *N*-acetyl-GCGK-βAla-FAKLAARLYRKA-NH_2 was utilized (heparin-binding domain underlined) (Sakiyama-Elbert and Hubbell, 2000a, 2000b; Tyler-Cross et al., 1994).

PEG-*bis*-Vinylsulfone Synthesis

PEG-*bis*-vinylsulfone was purchased from Shearwater Polymers (Huntsville, AL) or synthesized as follows. Divinylsulfone (1.2 mL; Fluka, Buchs, Switzerland) was dissolved with stirring in 25 mL triethanolamine buffer (2.2 mL triethanolamine/L, HCl to pH 8.0). Separately, 1 g PEG-dithiol (Shearwater Polymers) was dissolved in 25 mL triethanolamine buffer. Promptly the PEG-dithiol solution was added drop-wise into the divinylsulfone solution and stirred for 1–2 h at RT. The aqueous solution was washed twice with 150 mL diethyl ether and then freeze-dried. In two cycles the PEG-*bis*-vinylsulfone was dissolved in a minimal volume of dichloromethane, filtered, precipitated in diethyl ether cooled in an ice bath, collected by vacuum filtration, and dried in vacuo. The PEG-*bis*-divinylsulfone was then dissolved in water, sterile filtered, and freeze-dried yielding 0.81 g. ^{1}H NMR ($CDCl_3$): 3.64 ppm (156.46 H, PEG backbone), 6.34 ppm (m, 1.90 H, $=CH_2$), 6.71 ppm (m, 1.06 H, $-SO_2CH=$). Degree of vinylation: 97%.

Plasmin Substrate Characterization

Due to the analytical complexities of characterizing the kinetics of plasmin degradation of the peptide substrate in the gel phase, a variety of soluble analogs were synthesized and characterized. Thus, the crosslinking tricysteine substrate (GCYKNRCGYKNRCG-NH_2), containing two plasmin substrates (underlined), was replaced by a non-crosslinking dicysteine substrate (GCYKNRDCG), containing only one plasmin substrate. Enzyme-substrate kinetic

Table II. Plasmin cleavage sites in fibrin(ogen).[a]

P3	P2	P1	P1′	P2′	P3′	Chain P1	Reference
Leu	Ile	Lys	Met	Lys	Pro	α206	Hantgan et al., 1994; Takagi and Doolittle. 1975b
Asn	Phe	Lys	Ser	Gln	Leu	α219	Takagi and Doolittle, 1975b
Glu	Trp	Lys	Ala	Leu	Thr	α230	Takagi and Doolittle, 1975b
Thr	Gln	Lys	Lys	Val	Glu	β53	Takagi and Doolittle, 1975b
Leu	Ile	Lys	Ala	Ile	Gln	γ62	Takagi and Doolittle, 1975a; Nomura et al., 1993
Arg	Gln	Lys	Gln	Val	Lys	β130	Hantgan et al., 1994
Ser	Arg	Lys	Met	Leu	Gln	γ88	Hantgan et al., 1994
Ser	Tyr	Lys	Met	Ala	Asp	α583	Standker et al., 1995
Gln	Val	Lys	Asp	Asn	Gln	β133	Nomura et al., 1993
Thr	Leu	Lys	Ser	Arg	Lys	γ85	Hantgan et al., 1994; Takagi and Doolittle, 1975a
Tyr	Gln	Lys	Asn	Asn	Lys	α78	Takagi and Doolittle, 1975a

[a]The cleavage sites are listed approximately in the order in which they are cleaved upon exposure of fibrin(ogen) to plasmin.

Table III. Hydropathic indices for Lys-cleavage sites in fibrin(ogen).[a]

P3	P2	P1	P1′	P2′	P3′	P4′	GRAVY
Cys	Ile	Lys	Met	Lys	Pro	Cys	0.286
Cys	Phe	Lys	Ser	Gln	Leu	Cys	0.486
Cys	Trp	Lys	Ala	Leu	Thr	Cys	0.729
Cys	Gln	Lys	Lys	Val	Glu	Cys	−0.800
Cys	Ile	Lys	Ala	Ile	Gln	Cys	1.200
Cys	Gln	Lys	Gln	Val	Lys	Cys	−0.800
Cys	Arg	Lys	Met	Leu	Glu	Cys	−0.171
Cys	Tyr	Lys	Met	Ala	Asp	Cys	0.000
Cys	Val	Lys	Asp	Asn	Glu	Cys	−0.743
Cys	Leu	Lys	Ser	Arg	Lys	Cys	−0.614
Cys	Gln	Lys	Asn	Asn	Lys	Cys	−1.900

[a]P2-P3′ are derived from sequences in fibrin(ogen). P3 and P4′ form the reactive cassette for coupling to PEG-*bis*-vinylsulfone.

studies were carried out on the following derivatives to characterize the plasmin-sensitivity of the peptide in various molecular environments: (1) the peptide GCYKNRDCG, (2) the same peptide with the cysteines blocked with acetamide, (3) and the same peptide with the cysteines coupled to PEG. Iodoacetamide was dissolved (1.1 mg/mL) in HEPES-buffered saline (50 mM HEPES (13.02 g/L), 137 m*M* NaCl (8.0 g/L)), pH 8.0, and was mixed with the dicysteine peptide in HEPES-buffered saline, pH 8.0, at a 3:1 molar ratio of iodoacetamide to cysteine. The solution was stirred at RT, and the extent of reaction was monitored by analytical C18 chromatography (Nova-Pak, 3.9 × 150 mm column, Waters) until completion (30–60 min). Preparative C18 chromatography was used to purify the derivatized peptide, and MALDI-TOF was used to confirm the molecular mass. To form the diPEG-grafted peptide, PEG-monovinylsulfone (30 mg; Fluka) was dissolved in 1 mL HEPES-buffered saline, pH 8.0, to which 1 mg dicysteine peptide was added in 1 mL HEPES-buffered saline, pH 8.0. The solution was stirred at RT and the extent of reaction was monitored by analytical size exclusion chromatography (Shodex OHpak SB-802HQ, 8 × 300 mm column) until completion (1 h).

Plasmin-substrate degradation was followed chromatographically, and kinetic parameters were determined using Lineweaver-Burke plots. Substrates were dissolved in 50 m*M* HEPES-buffered saline, pH 7.4, and warmed to 37°C. Plasmin (porcine, 1 U/mL, Sigma) or collagenase (bacterial, type 4, 1 U/mL; Worthington Biochemical Corporation) in PBS, pH 7.4, was added under stirring. Samples were withdrawn over time, and the reaction was quenched by addition of acetic acid and storage at 4°C. The fraction of peptide cleaved in each sample was determined by analytical chromatography, using C18 chromatography for the peptide and the iodoacetamide-derivatized peptide, and using size-exclusion chromatography for the PEG-derivatized peptide.

Three-Dimensional Fibroblast Culture

Human fibrinogen (low plasminogen, Fluka) was dialyzed to exchange salts and diluted to give 2 mg fibrinogen/mL in Tris-buffered saline (28 m*M* Tris HCl (4.36 g/L), 5 m*M* Tris (0.64 g/L), 137 m*M* NaCl (8.0 g/L), 3 m*M* KCl (0.2 g/L); pH 7.4). Thrombin (human, Sigma T6884, 20 units/mL) in phosphate-buffered saline (3 m*M* KCl (0.2 g/L), 2 m*M* KH_2PO_4(0.2 g/L), 8 m*M* Na_2HPO_4 (2.16 g/L), 137 m*M* NaCl (8.0 g/L), pH 7.4) was added to the fibrinogen to give 0.25 unit thrombin/mL fibrinogen solution. Without delay, this solution was added to human foreskin fibroblasts (Clonetics, Walkersville, MD) to yield 3.3×10^7 cells/mL, and then 1.5–2 μL droplets of cells and fibrin were pipetted onto sterile silylated (SigmaCote; Sigma, used according to supplier's instructions) glass cover slips. The fibrin was allowed to polymerize for 20–30 min at 37°C in a humidified chamber with 5% CO_2. Fibrin-clotted fibroblasts were cultured within 25 μL hydrogels in 12-well tissue culture plates with 1 mL/well of Dulbecco's modified Eagle medium (DMEM) containing 10% fetal bovine serum and 1% antibiotic/antimycotic (Gibco/Life Technologies).

Hydrogel Formation

For cell culture within hydrogels, 15.8 mg PEG-divinylsulfone were dissolved in 110 μL HEPES-buffered saline, pH 7.6, added to monocysteine-RGD or -R*DG* peptide, and after 1 min to 4.3 mg tricysteine crosslinking peptide. The maximum RGD used in the precursor solution was 1.2 mg (10 m*M*); in samples with lower RGD concentrations, *N*-acetyl-cysteine was substituted on a molar basis to maintain constant modification of 1/10 vinylsulfones in all samples. Four well-spaced 25 μL drops of precursor solution were pipetted onto a sterile silylated glass slide. With forceps, one fibrin clot containing fibroblasts was transferred into each drop of hydrogel precursor. A Teflon® rectangle (700 μm thick) was placed at each end of the slide without touching the samples. A second silylated glass slide was clamped with binder clips over the lower slide. Samples were cured in this mold for 1 h at 37°C in a humidified chamber with 5% CO_2. Samples were then transferred to individual wells of a 12-well culture plate containing 1 mL of medium. Medium changes were performed at 1–2 h, 24 h, 4 d, 7 d, and then continuing twice a week.

Materials for calvarial implantation were made similarly to those for cell culture as described above, but with no cells, with 10 m*M* RGD, with BMP-2, in 20 μL aliquots, and with post-cure storage in PBS. Calvarial implants containing a heparin-based BMP-2 delivery system, also contained 1 mol heparin (average MW 18,000; Sigma H-9399) per mol of BMP monomer and 100 mol *N*-acetyl-GCGK-βAla-FAKLAARLYRKA-NH_2 (Tyler-Cross et al., 1994) per mol of heparin.

For stability and enzymatic degradation studies in the absence of cells, hydrogels were formed as for cell culture, but without RGD, from 6 mg of PEG-divinylsulfone dissolved with 90 μL HEPES-buffered saline, pH 7.6, and added to 1.8 mg of tricysteine peptide. For gel-degradation studies, 10 mg/mL Blue dextran (2,000,000 Da; Sigma) was physically incorporated to improve gel visibility. In all cases, the molar ratio of vinylsulfone to reduced cysteine was 1:1 in the initial precursor solution. Images were analyzed with a Leica Qwin image analysis software package.

Mechanical Characterization

Gelation behavior was studied using small-strain oscillatory shear experiments with a Bohlin CVO 120 High Resolution rheometer and plate–plate geometry in a humid atmosphere. Amplitude sweeps of the precursor solutions were first performed to determine the frequency and strain parameters where one could operate within the linear viscoelastic regime of the precursors. Precursor solutions (60 μL total)

were applied to the bottom plate. The upper plate (2-cm diameter) was then lowered to a measuring gap of 100 μm. After a short pre-shear period, the dynamic oscillating measurement was made using the autostress mode. The evolution of the storage and loss moduli at a constant frequency of 2.5 Hz were recorded.

Animal Experimentation and Analysis

Adult female Sprague-Dawley albino rats (300–350 g) were placed and maintained under general anesthesia (Halothane). The implant site was shaved and prepared with Betadine. A linear incision was made from nasal bone to the midsagital crest. Soft tissues were reflected, and the periosteum was dissected from the site, specifically from the occipital, frontal, and parietal bones. An 8-mm diameter craniotomy defect was created in the parietal bone with a dental handpiece. The calvarial disk was dissected away while avoiding dural perforations. The surgical site was flushed with saline to remove bone debris. A preformed sample disk of 8 mm was placed into the defect. The wound was closed by closing the soft tissues with skin staples. Before waking, animals were given analgesia. The animals were asphyxiated 21 days after implantation. Explants were radiographed with a dental radiography unit and dental films. Explants were analyzed by micro-computed tomography on a μCT 40 imaging system (Scanco Medical, Bassersdorf, Switzerland) providing an isotropic resolution of 18 μm. A constrained Gaussian filter was used to partly suppress the noise in the volumes. Mineralized bone tissue was segmented from nonmineralized tissue using a global thresholding procedure (Muller and Ruegsegger, 1997). All samples were binarized using the same parameters for the filter width (1.2), the filter support (1) and the threshold (224; in permille of maximal image gray value, corresponds to an attenuation coefficient of 1.8 cm^{-1}). Three-dimensional visualizations were created using in-house software for surface triangulation and rendering (Muller et al., 1994; Muller and Ruegsegger, 1997). Samples were sequentially dried, defatted, fixed, and embedded. Sections (5 μm) were stained with Toluidine blue O and Goldner Trichrome. At all steps the surgeon was blinded with regard to treatment. Five animals were used per treatment grouping.

Statistics

Values are given as means ± average deviations. *P* values were calculated using a two-tailed, nonpaired Student's *t*-test.

RESULTS AND DISCUSSION

Protease Sensitivity

We synthesized the highly soluble crosslinking peptide, GCYKNRCGYKNRCG-NH_2, such that there was a plasmin-sensitive sequence (underlined), between each crosslinking site (cysteine, C). Enzyme-substrate kinetic studies were carried out on the peptide itself, on the peptide with the thiol of the Cys residues blocked, and on the peptide with the thiol of the each Cys residue grafted to PEG. This allowed exploration of the effect of the chemical and steric environment on the plasmin-sensitivity of the selected peptide. For the dicysteine peptide itself, the Michaelis constant (K_m) was calculated to be 446 ± 5 μ*M* (Mean ± SEM) and the turnover number 319 ± 7 s^{-1}. When the cysteine thiols blocked by reaction with a small molecule, the K_m value decreased to 188 ± 58 μ*M* but also the turnover number to 178 ± 16 s^{-1}. When the peptide was covalently bound to the much larger PEG as a soluble model of the peptide contained in the PEG network, a K_m of 640 μ*M* and a turnover number of 5 s^{-1} were measured. Even in this somewhat sterically hindered environment, the turnover rate for plasmin cleavage is of the same order of magnitude as for uncrosslinked fibrin (Anand et al., 1995). When the peptide was formed using *D* rather than *L* stereoisomers of lysine and arginine, no cleavage by plasmin was observed over 27 h, and when collagenase rather than plasmin was used, likewise no cleavage was observed over 27 h.

Hydrogel Formation and Stability

We transformed telechelic PEG-*bis*-vinyl sulfone, dissolved in buffered saline, into an insoluble hydrogel by conjugate addition with the tricysteine crosslinking peptide. The kinetics of this conversion, as well as the physical and enzymatic characteristics of the materials, were studied. The gel point was defined as the time at which the phase angle was equal to 45°, e.g., the crossover point of the elastic (G′) and loss (G″) rheometric moduli. In a pH range of physiological relevance, materials containing 0.1 g/mL PEG in the precursor solution gelled in 5.4 ± 0.9 min at pH 7.0 and 2.0 ± 0.3 min at pH 8.2 at 25°C. This pH dependence of the gelation rate in the vicinity of the pK_a of the cysteine thiol agrees with the expectation that the addition rate depends on the deprotonation of the thiol (Lutolf et al., 2001). After 60 ± 20 min reaction, the materials reached a plateau G′ of 10,800 ± 2700 Pa. This value compares favorably with values typically observed with natural wound healing matrices, such as fibrin (Clark and Ross-Murphy, 1987). After 4 h in aqueous solution, gels reached an equilibrium swollen volume 2.5 times their initial volume, to result in a PEG concentration of approximately 5% (mass/volume). Hydrogel materials (50 μL; stored at 37°C in phosphate buffered saline at pH 7.4 and containing 0.1% sodium azide) were sufficiently stable against passive hydrolysis and reversibility of the addition reaction to demonstrate no macroscopic loss of mechanical properties for at least 4 months, a time scale significantly longer than expected biological remodeling in vitro or in vivo. Gels exposed to 10 units/mL collagenase resisted hydrolysis for more than 2 d, as measured by their constant volume and mechanical properties. In contrast, gels exposed to 0.1 unit/mL

plasmin were completely degraded in 4–5 h. Gels prepared with the crosslinking peptide containing the *D* rather than *L*-stereoisomers of lysine and arginine were not degraded by 1.0 unit/mL plasmin in 2 d.

Materials Response In Vitro

We first studied the cellular response to the novel hydrogels with human fibroblasts. We formed hydrogels in contact with fibrin-entrapped cells such that the cells were completely surrounded by the crosslinked synthetic hydrogel. In addition to sensitivity to plasmin, as described above, we incorporated cell adhesion character by prereacting a fraction of PEG-*bis*-vinyl sulfone with the single cysteine residue in *N*-acetyl-G**C**GYGRGDSPG-NH_2 prior to crosslinking. In such gels, we observed outgrowth of human fibroblasts from the fibrin clots into the colorless, transparent PEG-based network. Fibroblasts assumed a spindle-shaped morphology as they extended and migrated into the synthetic hydrogels within a 3D-culture environment (Fig. 1). These cells could easily be distinguished from cells that, when incompletely surrounded by hydrogel, grew out on the surfaces of the hydrogels and assumed a spread morphology. In three dimensions, fibroblasts not only extended processes into the degradable hydrogels, but also whole cells migrated into the materials as observed by live cell nuclear staining, which stained nuclei far from the fibrin clot (not shown). It may thus be concluded that the hydrogel matrix that was both adhesive and plasmin-sensitive provided adequate adhesion and underlying mechanical properties required to permit cellular outgrowth.

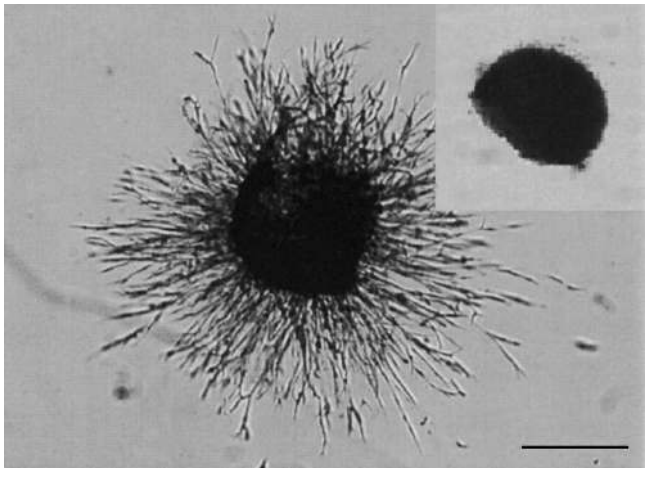

Figure 1. Fibroblast outgrowth from a fibrin clot into synthetic hydrogels formed in situ. Fibroblasts assume a spindle-shaped morphology as they migrate three-dimensionally within a synthetic hydrogel containing plasmin-degradable crosslinks and cell-adhesive RGD peptide ligands. Day 7. Scale bar = 500 μm. Differential interference contrast microscopy. Inset: Migration was not observed, when cells were entrapped in a plasmin-insensitive hydrogel, obtained by substitution of *D*- for *L*-lysine and arginine at the plasmin cleavage site.

We measured the projected area of the halo of 3D outgrowth from the fibrin clot as a function of time and calculated an area-averaged cell migration distance as the radius of an annulus. In materials containing both a plasmin-sensitive peptide crosslinker and pendant RGD peptide at the maximum RGD concentration tested, the outgrowth persisted for 11–14 d at an average rate of 67 ± 18 μm/d. Beyond this duration, material degradation was so significant as to lead to mechanical instability of the materials and termination of the experiments. This was probably due to the absence within the materials of protease inhibitors, which are naturally present in vivo. Material degradation and 3D cell migration could be slowed by addition of exogenous inhibitors of fibrinolysis, such as ϵ-aminocaproic acid, which inhibits plasmin activity (Herbert et al., 1996) (Fig. 2). Conversely, addition of a growth factor that up-regulates the plasminogen activation pathway, FGF-2 or PDGF-BB (Fibbi et al., 1999), increased the rate of cell migration within the synthetic plasmin-sensitive materials, demonstrating that the rate of material remodeling is controlled by cellular influences.

In materials where we replaced the plasmin-degradable crosslinking peptide with the plasmin-insensitive crosslinker containing the *D* rather than natural *L*-stereoisomers

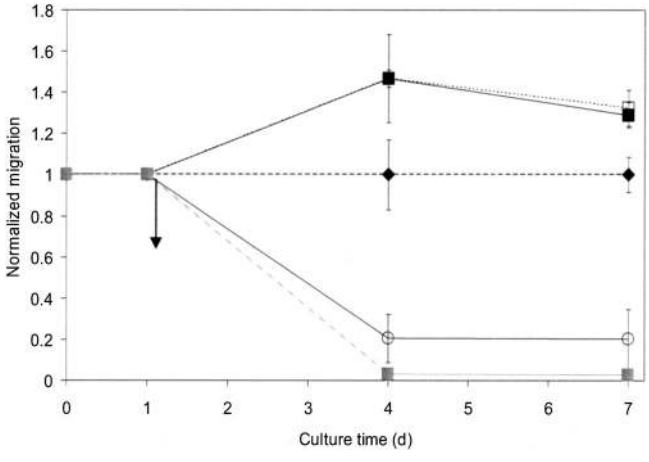

Figure 2. Dependence of fibroblasts on plasmin activity when migrating through synthetic hydrogels. Clot-embedded fibroblasts were cultured within synthetic matrices. After 1 d of culture, modulators of plasmin activity were added to plasmin-degradable samples (↓). Migration distances were normalized to controls (-◆-) in which no modulator of the plasmin pathway was added to cells cultured in plasmin-sensitive matrices. In materials crosslinked with peptides containing *D* amino acids, fibroblasts were not able to migrate out of the fibrin clots and into the hydrogels (—■—). Addition of ϵ-aminocaproic acid (200 m*M*; Sigma) inhibited fibroblast migration distance by 80% at days 4 and 7 in 3D culture within plasmin-sensitive hydrogels ($p < 0.05$; —○—). FGF-2 (10 ng/mL, recombinant human, PeproTech, London, England; --□--) and PDGF-BB (10 ng/mL, recombinant human, PeproTech, —■—) each independently increased the rate of cell migration in synthetic plasmin-degradable hydrogels by more than 25% ($p < 0.05$). In the case of growth factor-containing samples, aphidicolin (2 μg/mL), an inhibitor of DNA polymerase-α, was added to controls and treated samples to prevent the increased cell proliferation induced by the growth factors that was the cause of increased cell migration.

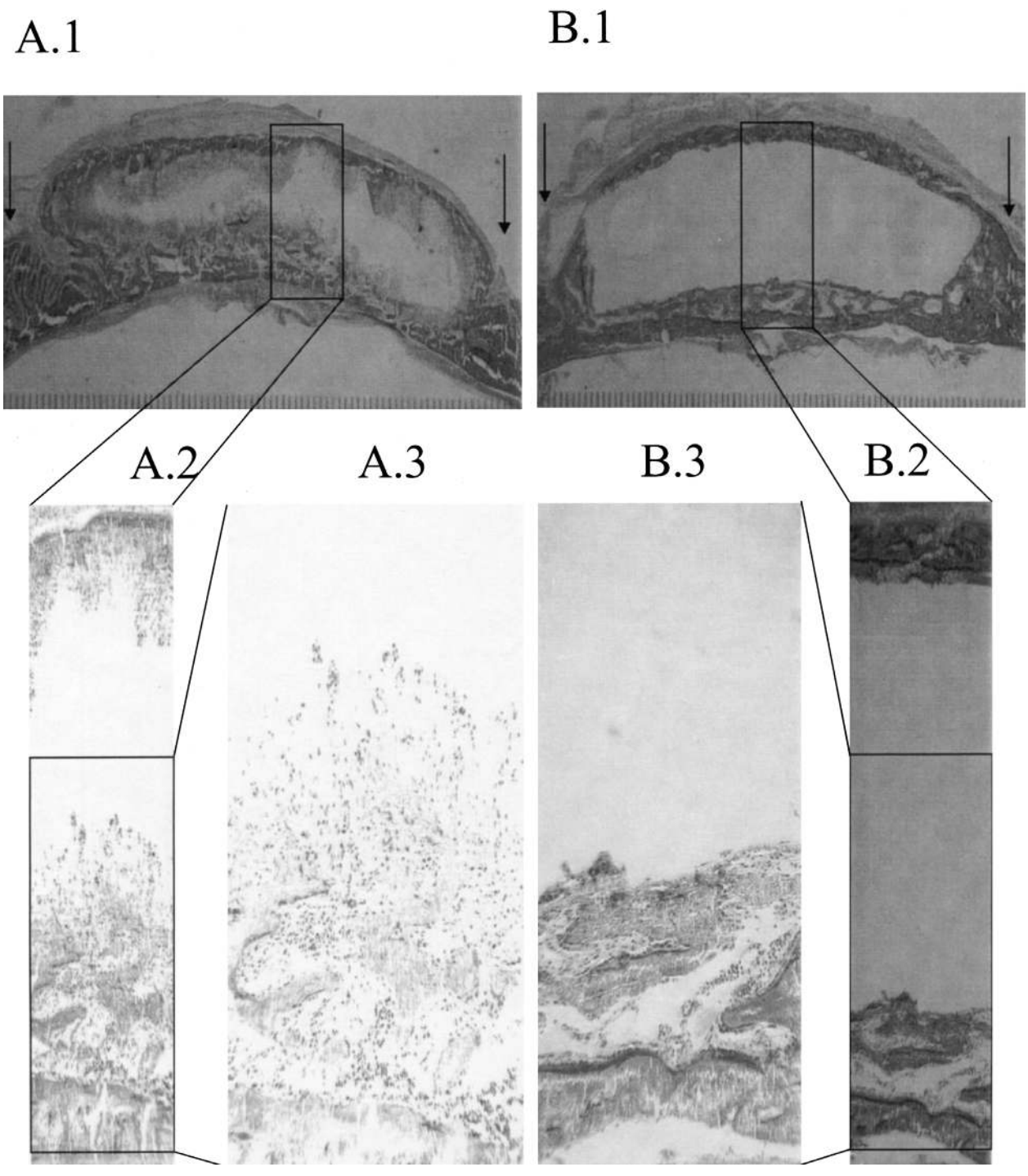

Figure 3. Process of bone healing shown histologically. Cross-section of defect 3 weeks after synthetic material implantation, showing typical sections. The defect margins, 8 mm apart, are indicated (↓). Cell encapsulation of and migration into the implant were observed. (A) In animals treated with BMP-2 in a matrix that was adhesive, plasmin-sensitive and contained heparin binding sites for BMP-2, calcified bone (dark green) formation was observed around and within the implant, following a wave of cell infiltration progressing toward the center of the implant (more easily seen in the higher magnifications). Osteoblasts (fuschia) are observed at the osteoid interface between the newly deposited calcified bone. (B) In animals treated as in (A) but with a plasmin-insensitive matrix, bone formation was limited to the surface of the implant and cell infiltration within the material was not observed.

of lysine and arginine, no significant migration of fibroblasts into the synthetic hydrogels was observed (Fig. 1, inset and Fig. 2). Decreasing the concentration of RGD within plasmin-sensitive materials decreased the rate and extent of cell migration in a concentration dependent manner (not shown). Exchanging the RGD peptide for an inactive RDG peptide (Pierschbacher and Ruoslahti, 1984) significantly decreased the amount of fibroblast outgrowth and migration into the hydrogel (74% $\pm$ 6% inhibition averaged for all time points). These observations indicate that both enzymatic degradability and specifically mediated cell adhesion are required for cell migration within the 3D matrices.

Materials Response In Vivo

To study the biological response to the newly designed materials, we used the matrices as carriers for recombinant human bone morphogenetic protein-2 (BMP-2), which was noncovalently incorporated during gel crosslinking. We implanted hydrogel disks (8 mm) in critical size calvarial defects of the same size in rats, a standard model in bone regeneration studies (Einhorn, 1999; Schmitz and Hollinger, 1986). We selected an early time point, 3 weeks, for sacrifice and analysis of the implants to allow observation of both cell invasion and mineralization during healing. At time of explantation, the treated regions were radiographed, analyzed by micro-computed tomography, and histologically processed.

Histology demonstrated a wave of infiltration by host cells into plasmin-degradable materials (Fig. 3A), consistent with specific, local, cell-mediated degradation. In places, the cellular infiltrate was observed to cross the entire thickness of the implant at 3 weeks (Fig. 3A.1, middle) and in other regions to infiltrate half of its thickness; cellular infiltration was observed to occur into the gel network in multicellular finger-like processes, consistent with a hypothesis of infiltration inducing degradation (Fig. 3A.2–3). When a plasmin-insensitive gel network was studied, we did not observe cellular infiltration within the material (Fig. 3B).

We also analyzed the explanted samples for mineralization, both histologically and radiographically. At a dose of 5 μg BMP-2 per implant, we saw intramembraneous bone formation around and within the plasmin-sensitive implants (Fig. 3A), but only around the plasmin-insensitive implants (Fig. 3B). We used radiography to determine the extent of covering of the cranial defect with new bone. When BMP-2 was incorporated into plasmin-sensitive hydrogels containing both heparin and a covalently bound heparin-binding peptide to together serve as a growth factor delivery system, new bone covered 94% of the defect area (averaged across all animals in the treatment groupings; Fig. 4A and B), and the radio-opacity was 84% of that of neighboring, uninjured bone after 3 weeks. Control materials, either containing no BMP-2 or containing a plasmin-insensitive crosslinker (Fig. 4C), showed little bone formation (Fig. 4A and 4C). Micro-computed tomography was used to gain more insight into the morphology of bone regeneration. When we analyzed samples that contained BMP-2 but were insensitive to plasmin, we never observed mineralization other than at the surface of the implant (Fig. 4D), while when a plasmin-sensitive gel network was employed we observed occasional mineralization into the depths of the implant, even at the early time point of 3 weeks (Fig. 4E).

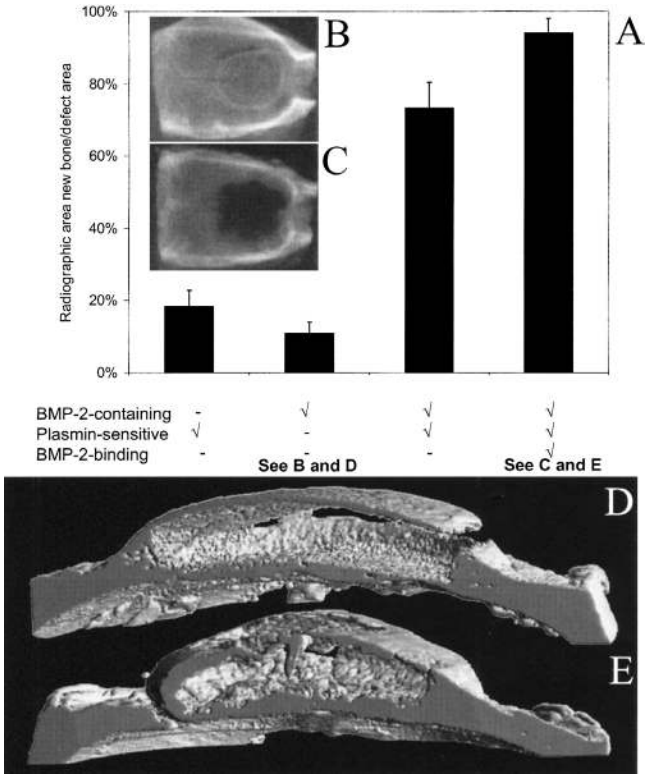

Figure 4. (A) Area of new bone at 3 weeks measured radiographically. In animals receiving implants without BMP-2 or without plasmin degradable crosslinks, bone formation was observed only at the wound margins. In animals receiving implants containing BMP-2 and plasmin-degradable crosslinks, an average of 73% ± 7% of the defect area was covered with new bone. When heparin and a heparin-binding peptide were incorporated to better retain the BMP-2 within the materials, an average of 94% ± 4% of the defect area was covered (significantly different than all other treatments; $p < 0.02$). (B and C) Typical radiography of typical crania with BMP-2 treatment from a plasmin-sensitive (B) and plasmin-insensitive (C) matrix. (D and E) Three-dimensional projections of micro-computed tomographic images of typical crania with BMP-2 treatment from a plasmin-sensitive (D) and plasmin-insensitive (E) matrix showed bone formation only around the plasmin-insensitive material, while bone formation penetrated into the plasmin-sensitive materials.

CONCLUSION

In the present work, we report on totally synthetic, biomimetic hydrogel materials that promote cell adhesion to incorporated ligands and degrade as designed in response to cell-regulated local fibrinolytic activity. Synthetic and surgical simplicity was afforded by use of the conjugate addition reaction to form the materials in situ from two liquid precursors at room temperature (Elbert and Hubbell, 2001; Elbert et al., 2001; Lutolf and Hubbell, 2003; Lutolf et al., 2003; Lutolf et al., 2001). We have incorporated binding sites for growth factors and have demonstrated that these factors induce morphogenesis, in this case bone regeneration, using the potent bone-forming capacity of BMP-2 (Reddi, 2000; Ripamonti and Reddi, 1997; Urist et al., 1987; Wozney, 1995; Yamaguchi et al., 1996); the benefits of the matrix-bound vs. free BMP-2 were statistically observable. Such cell-responsive materials permit the time scale of material degradation and growth factor delivery to depend on local endogenous processes of morphogenesis; this responsiveness of the material to the local healing response is important because morphogenesis rates vary due to the site of implantation, the nature of a wound, and the indi-

vidual patient. The fully synthetic nature of these materials permits flexibility in design of the mechanical properties as well as adhesion to and degradability of the materials, all without the problems associated with animal- or human-derived materials (European Agency for the Evaluation of Medicinal Products, 2001). Furthermore, the results presented here show that the design of synthetic materials with the appropriate biomimetic character permits controlled engineering, even entirely in situ, of tissues de novo.

We thank D.L. Elbert and H. Hall for helpful discussions, S. vandeVondele and the Protein Service Laboratory of the ETH for mass spectrometry, J.C. Schense for his assistance with the cra-nial surgery.

References

Abuchowski A, McCoy JR, Palczuk NC, Vanes T, Davis FF. 1977. Effect of covalent attachment of polyethylene-glycol on immunogenicity and circulating life of bovine liver catalase. J Biol Chem 252:3582–3586.

Anand S, Wu JH, Diamond SL. 1995. Enzyme-mediated proteolysis of fibrous biopolymers—dissolution front movement in fibrin or collagen under conditions of diffusive or convective-transport. Biotechnol Bioeng 48:89–107.

Backes BJ, Harris JL, Leonetti F, Craik CS, Ellman JA. 2000. Synthesis of positional-scanning libraries of fluorogenic peptide substrates to define the extended substrate specificity of plasmin and thrombin. Nat Biotechnol 18:187–193.

Chang C, Werb Z. 2001. The many faces of metalloproteases: Cell growth, invasion, angiogenesis and metastasis. Trends Cell Biol 11:S37–S43.

Chen W. 1992. Membrane proteases: Roles in tissue remodeling and tumour invasion. Curr Opin Cell Biol 4:802–809.

Clark AH, Ross-Murphy SB. 1987. Structural and mechanical-properties of bio-polymer gels. Adv Polym Sci 83:57–192.

Dearfield KL, Harrington-Brock K, Doerr CL, Rabinowitz JR, Moore MM. 1991. Genotoxicity in mouse lymphoma-cells of chemicals capable of Michael addition. Mutagenesis 6:519–525.

Einhorn TA. 1999. Clinically applied models of bone regeneration in tissue engineering research. Clin Orthop Rel Res:S59–S67.

Elbert DL, Hubbell JA. 2001. Conjugate addition reactions combined with free-radical cross-linking for the design of materials for tissue engineering. Biomacromol 2:430–441.

Elbert DL, Pratt AB, Lutolf MP, Halstenberg S, Hubbell JA. 2001. Protein delivery from materials formed by self-selective conjugate addition reactions. J Control Rel 76:11–25.

European Agency for the Evaluation of Medicinal Products. 2001. CPMP/0393/01, www.eudra.org/humandocs/humans/epar/osteogenicprot1/osteogenicprot1.htm.

Fibbi G, Pucci M, Grappone C, Pellegrini G, Salzano R, Casini A, Milani S, Del Rosso M. 1999. Functions of the fibrinolytic system in human ito cells and its control by basic fibroblast and platelet-derived growth factor. Hepatology 29:868–878.

Friedlaender GE, Perry CR, Cole JD, Cook SD, Cierny G, Muschler GF, Zych GA, Calhoun JH, LaForte AJ, Yin S. 2001. Osteogenic protein-1 (bone morphogenetic protein-7) in the treatment of tibial nonunions—A prospective, randomized clinical trial comparing rhOP-1 with fresh bone autograft. J Bone Joint Surg-Am 83A:S151–S158.

Gobin AS, West JL. 2002. Cell migration through defined, synthetic extracellular matrix analogues. Faseb J 16:U1–U16.

Hantgan RR, Francis CW, Marder VJ. 1994. Fibrinogen structure and physiology. In: Colman RW, Hirsh J, Marder VJ, Saltzman EW, editors. Hemostasis and thrombosis: Basic principles and clinical practice, 3rd ed. Philadelphia: Lippincott Company.

Harris JM. 1992. Introduction to biotechnical and biomedical applications of poly(ethylene glycol). In: Harris JM, editor. Poly(ethylene glycol) chemistry, biotechnical and biomedical applications. New York: Plenum Press.

Herbert CB, Bittner GD, Hubbell JA. 1996. Effects of fibrinolysis on neurite growth from dorsal root ganglia cultured in two- and three-dimensional fibrin gels. J Comp Neurol 365:380–391.

Hern DL, Hubbell JA. 1998. Incorporation of adhesion peptides into nonadhesive hydrogels useful for tissue resurfacing. J Biomed Mater Res 39:266–276.

Horch RE, Bannasch H, Stark GB. 2001. Transplantation of cultured autologous keratinocytes in fibrin sealant biomatrix to resurface chronic wounds. Transplant Proc 33:642–644.

Howe A, Aplin AE, Alahari SK, Juliano RL. 1998. Integrin signaling and cell growth control. Curr Opin Cell Biol 10:220–231.

Howell TH, Fiorellini J, Jones A, Alder M, Nummikoski P, Lazaro M, Lilly L, Cochran D. 1997. A feasibility study evaluating rhBMP-2 absorbable collagen sponge device for local alveolar ridge preservation or augmentation. Int J Periodontics Restor Dent 17:125–139.

Hunziker EB, Quinn TM, Hauselmann HJ. 2002. Quantitative structural organization of normal adult human articular cartilage. Osteoarthritis Cartilage 10:564–572.

Huttenlocher A, Sandborg RR, Horwitz AF. 1995. Adhesion in cell-migration. Curr Opin Cell Biol 7:697–706.

Kiel B. 1992. Specificity of proteolysis. New York: Springer Verlag.

Kyte J, Doolittle RF. 1982. A simple method for displaying the hydropathic character of a protein. J Mol Biol 157:105–132.

Lu L, Peter SJ, Lyman MD, Lai HL, Leite SM, Tamada JA, Uyama S, Vacanti JP, Langer R, Mikos AG. 2000. In vitro and in vivo degradation of porous poly(DL-lactic-co- glycolic acid) foams. Biomaterials 21:1837–1845.

Lutolf MP, Hubbell JA. 2003. Synthesis and physicochemical characterization of end-linked poly(ethylene glycol)-co-peptide hydrogels formed by Michael-type addition. Biomacromolec 4:713–722.

Lutolf MP, Lauer-Fields JL, Schmoekel HG, Metters AT, Weber FE, Fields GB, Hubbell JA. 2003. Synthetic matrix metalloproteinase-sensitive hydrogels for the conduction of tissue regeneration: Engineering cell-invasion characteristics. Proc Natl Acad Sci USA 100:5413–5418.

Lutolf MP, Tirelli N, Cerritelli S, Cavalli L, Hubbell JA. 2001. Systematic modulation of Michael-type reactivity of thiols through the use of charged amino acids. Bioconjugate Chem 12:1051–1056.

Maheshwari G, Brown G, Lauffenburger DA, Wells A, Griffith LG. 2000. Cell adhesion and motility depend on nanoscale RGD clustering. J Cell Sci 113:1677–1686.

Massia SP, Hubbell JA. 1991. An RGD spacing of 440nm is sufficient for integrin alpha-V- beta-3-mediated fibroblast spreading and 140nm for focal contact and stress fiber formation. J Cell Biol 114:1089–1100.

Morpurgo M, Veronese FM, Kachensky D, Harris JM. 1996. Preparation and characterization of poly(ethylene glycol) vinyl sulfone. Bioconjugate Chem 7:363–368.

Muller R, Hildebrand T, Ruegsegger P. 1994. Noninvasive bone-biopsy—A new method to analyze and display the 3-dimensional structure of trabecular bone. Phys Med Biol 39:145–164.

Muller R, Ruegsegger P. 1997. Micro-tomographic imaging for the nondestructive evaluation of trabecular bone architecture. Stud Health Technol Infor 40:61–79.

Murphy G, Gavrilovic J. 1999. Proteolysis and cell migration: Creating a path? Curr Opin Cell Biol 11:614–621.

Nomura S, Kashiwagi S, Ito H, Mimura Y, Nakamura K. 1993. Degradation of fibrinogen and fibrin by plasmin and nonplasmin proteases in the chronic subdural-hematoma - evaluation by sodium dodecyl sulfate-polyacrylamide gel-electrophoresis and immunoblot. Electrophoresis 14:1318–1321.

Palecek SP, Loftus JC, Ginsberg MH, Lauffenburger DA, Horwitz AF. 1997. Integrin-ligand binding properties govern cell migration speed through cell-substratum adhesiveness. Nature 385:537–540.

Pierschbacher MD, Ruoslahti E. 1984. Cell attachment activity of fibronectin can be duplicated by small synthetic fragments of the molecule. Nature 309:30–33.

Reddi AH. 2000. Morphogenetic messages are in the extracellular matrix: Biotechnology from bench to bedside. Biochem Soc Trans 28:345–349.

Ripamonti U, Reddi AH. 1997. Tissue engineering, morphogenesis, and regeneration of the periodontal tissues by bone morphogenetic proteins. Crit Rev Oral Biol Med 8:154–163.

Ruppert R, Hoffmann E, Sebald W. 1996. Human bone morphogenetic protein 2 contains a heparin-binding site which modifies its biological activity. Eur J Biochem 237:295–302.

Sakiyama-Elbert SE, Hubbell JA. 2000a. Controlled release of nerve growth factor from a heparin- containing fibrin-based cell ingrowth matrix. J Control Release 69:149–158.

Sakiyama-Elbert SE, Hubbell JA. 2000b. Development of fibrin derivatives for controlled release of heparin-binding growth factors. J Control Release 65:389–402.

Schechter I, Berger A. 1967. On size of active site in proteases .I. Papain. Biochem Biophys Res Commun 27:157–162.

Schmitz JP, Hollinger JO. 1986. The critical size defect as an experimental-model for craniomandibulofacial nonunions. Clin Orthop Rel Res:299–308.

Shastri VP, Martin I, Langer R. 2000. Macroporous polymer foams by hydrocarbon templating. Proc Natl Acad Sci USA 97:1970–1975.

Sieron AL, Louneva N, Fertala A. 2002. Site-specific interaction of bone morphogenetic protein 2 with procollagen II. Cytokine 18:214–221.

Standker L, Sillard R, Bensch KW, Ruf A, Raida M, Schulzknappe P, Schepky AG, Patscheke H, Forssmann WG. 1995. In-vivo degradation of human fibrinogen a-alpha - detection of cleavage sites and release of antithrombotic peptides. Biochem Biophys Res Commun 215: 896–902.

Sternlicht MD, Werb Z. 2001. How matrix metalloproteinases regulate cell behavior. Ann Rev Cell Dev Biol 17:463–516.

Streuli C. 1999. Extracellular matrix remodeling and cellular differentiation. Curr Opin Cell Biol 11:634–640.

Takagi T, Doolittle RF. 1975a. Amino-acid sequence studies on alpha-chain of human fibrinogen—Location of 4 plasmin attack points and a covalent cross-linking site. Biochemistry 14:5149–5156.

Takagi T, Doolittle RF. 1975b. Amino-acid sequence studies on plasmin-derived fragments of human fibrinogen—Amino-terminal sequences of intermediate and terminal fragments. Biochemistry 14:940–946.

Tyler-Cross R, Sobel M, Marques D, Harris RB. 1994. Heparin-binding domain peptides of antithrombin-iii—Analysis by isothermal titration calorimetry and circular-dichroism spectroscopy. Protein Sci 3:620–627.

Urist MR, Nilsson O, Rasmussen J, Hirota W, Lovell T, Schmalzreid T, Finerman GAM. 1987. Bone regeneration under the influence of a bone morphogenetic protein (BMP) beta-tricalcium phosphate (TCP) composite in skull trephine defects in dogs. Clin Orthop Rel Res: 295–304.

Vu TH, Werb Z. 2000. Matrix metalloproteinases: Effectors of development and normal physiology. Genes & Development 14:2123–2133.

Wake MC, Patrick CW, Mikos AG. 1994. Pore morphology effects on the fibrovascular tissue-growth in porous polymer substrates. Cell Transplant 3:339–343.

Werb Z. 1997. ECM and cell surface proteolysis: Regulating cellular ecology. Cell 91:439–442.

West JL, Hubbell JA. 1999. Polymeric biomaterials with degradation sites for proteases involved in cell migration. Macromolec 32:241–244.

Wozney JM. 1995. The potential role of bone morphogenetic proteins in periodontal reconstruction. J Periodont 66:506–510.

Yamada Y, Kleinman HK. 1992. Functional domains of cell adhesion molecules. Curr Opin Cell Biol 4:819–823.

Yamaguchi A, Ishizuya T, Kintou N, Wada Y, Katagiri T, Wozney JM, Rosen V, Yoshiki S. 1996. Effects of BMP-2, BMP-4, and BMP-6 on osteoblastic differentiation of bone marrow-derived stromal cell lines, ST2 and MC3T3-G2/PA6. Biochem Biophys Res Commun 220: 366–371.